

Decoding cinnabarinic acid specific stanniocalcin 2 induction by aryl hydrocarbon receptor

Nikhil Y. Patil¹, Hui Tang², Iulia Rus¹, Kangling Zhang², Aditya D. Joshi^{1*}

¹Department of Pharmaceutical Sciences, University of Oklahoma Health Sciences
Center, Oklahoma City, Oklahoma 73117

²Department of Pharmacology and Toxicology, University of Texas Medical Branch,
Galveston, Texas 77555

Running Title: Agonist-specific differential gene regulation by liver AhR

Corresponding author: * Dr. Aditya D. Joshi, Department of Pharmaceutical Sciences, University of Oklahoma Health Sciences Center, 1110 N. Stonewall Ave., Oklahoma City, Oklahoma 73117, E-mail: aditya-joshi@ouhsc.edu

Number of Text Pages: 42

Number of Tables: 0

Number of Figures: 7 + 2 supplementary

Number of References: 67

Number of Words in the Abstract: 246

Number of Words in the Introduction: 481

Number of Words in the Discussion: 1334

Abbreviations: AhR, Aryl hydrocarbon receptor; Arnt, Aryl hydrocarbon receptor nuclear translocator; cyp1a1, cytochrome P450 family 1 member A1; stc2, stanniocalcin 2; TCDD, 2,3,7,8-tetrachlorodibenzo-p-dioxin; CA, cinnabarinic acid; XREs, xenobiotic response elements; H3 K14ac, Histone H3 lysine 14 acetylation; H3 K23ac, Histone H3 lysine 23 acetylation; H3 K27dime, Histone H3 lysine 27 dimethylation; H4 K5ac, Histone H4 lysine 5 acetylation; H3 K79me, Histone H3 lysine 79 methylation.

Abstract

Aryl hydrocarbon Receptor (AhR) is a ligand mediated transcription factor known for regulating response to xenobiotics, including prototypical 2,3,7,8-tetrachlorodibenzo-p-dioxin (TCDD) through the activation of cytochrome P450 1A1 (encoded by *cyp1a1*) expression. Upon ligand-binding AhR translocate to nucleus, interacts with AhR nuclear translocator (Arnt) and bind to xenobiotic response element(s) (GCGTG, XREs) present in the promoter region of AhR regulated genes. Recently, we identified a novel tryptophan catabolite, cinnabarinic acid (CA) as an endogenous AhR agonist capable of activating expression of AhR target gene, stanniocalcin 2 (*stc2*). The CA-driven *stc2* induction bestowed cytoprotection against hepatotoxicity in an AhR-dependent manner. Interestingly, only CA, but not TCDD was able to induce *stc2* expression in liver and CA was unable to upregulate the TCDD responsive *cyp1a1* gene. In this report, we identified CA-specific histone H4 K5 acetylation and H3 K79 methylation at AhR-bound *stc2* promoter. Moreover, histone H4 K5 acetylation writer, Atf2 and H3 K79 methylation writer, Dot1l were interacting with AhR-complex at *stc2* promoter exclusively in response to CA treatment concurrent with the histone epigenetic marks. Suppressing Atf2 and Dot1l expression using RNA interference confirmed their role in *stc2* expression. CRISPR/Cas9 assisted replacement of *cyp1a1* promoter encompassing XREs with *stc2* promoter XREs resulted in CA-dependent induction of *cyp1a1* underlining fundamental role of quaternary structure of XRE sequence in agonist-specific gene regulation. In conclusion, CA-driven recruitment of specific chromatin regulators to AhR complex and resulting histone epigenetic modifications may serve as a molecular basis for agonist specific *stc2* regulation by AhR.

Significance Statement

Results reported here provide a mechanistic explanation for the agonist-specific differential gene regulation by identifying interaction of AhR with specific chromatin regulators concomitant with unique histone epigenetic marks. This study also demonstrated that the agonist-specific target gene expression can be transferred with the gene-specific promoter XRE sequence in the context of chromatin architecture.

Introduction

The basic helix-loop-helix Per/Arnt/Sim domain family (bHLH-PAS) of transcription factors and regulators have distinct physiological, pathological and developmental functions despite conserved domain architecture (McIntosh et al., 2010). Within the family, the Aryl hydrocarbon Receptor (AhR) is a key transcription factor activated by number of xenobiotics including 2,3,7,8-tetrachlorodibenzo-p-dioxin (TCDD) (Hankinson, 1993; Hankinson, 1995; Legraverend et al., 1982; Nebert and Gelboin, 1968a; Nebert and Gelboin, 1968b; Nebert et al., 1993). In an unliganded state, AhR resides in the cytoplasm in complex with molecular chaperonins – heat shock protein 90 (hsp90), p23, and AhR interaction protein (AIP) (Flaveny et al., 2010; Ma et al., 2009). Upon TCDD binding, AhR dissociates from chaperonins, translocate to the nucleus, and heterodimerizes with Aryl hydrocarbon Receptor nuclear translocator (Arnt) (Fukunaga et al., 1995). The liganded AhR-Arnt complex then binds to Xenobiotic Response Elements (XREs, GCGTG motif) present in the promoter region of AhR target genes, including archetypical *cyp1a1* (Elferink et al., 1990; Elferink and Whitlock, 1990; Jones et al., 1986).

Since the discovery of AhR, wide range of xenobiotics including polycyclic aromatic hydrocarbons, halogenated aromatic hydrocarbons, polychlorinated biphenyls have been identified as exogenous AhR ligands (Nguyen and Bradfield, 2008). Additionally, recent advancement in the field included plethora of structurally diverse bacterial products, dietary and endogenous compounds as AhR agonists (Denison and Nagy, 2003; Denison et al., 2011; Hubbard et al., 2015). Among them, cinnabarinic acid (CA), a tryptophan metabolite and a byproduct of kynurenine pathway has been shown

to activate AhR (Lowe et al., 2014). Upon CA treatment, AhR-Arnt complex is directly recruited to the 8 XREs clustered in 218 bp region of stanniocalcin 2 (*stc2*) promoter (Harper et al., 2013). Interestingly, in hepatocytes only CA but not TCDD, induced *stc2* expression through an XRE-driven mechanism; whereas CA, in contrast to TCDD, did not upregulate *cyp1a1* expression (Harper et al., 2013; Joshi et al., 2015). The CA-driven AhR-dependent *stc2* upregulation was responsible for the protection against endoplasmic reticulum / oxidative stress – induced apoptosis both *in vitro* and *in vivo* (Joshi et al., 2015). To investigate the molecular basis for the agonist specific mutually exclusive transcription response, we previously employed mass spectrometry on immunoaffinity purified AhR complexes captured after CA or TCDD treatments (IP-MS) (Joshi et al., 2017). Mass spectrometry identified CA-specific interaction of AhR with metastasis-associated protein 2 (*Mta2*) – a known chromatin regulator, concomitant with histone H4 lysine 5 acetylation (*H4 K5ac*). Moreover, *H4 K5ac* was absolutely dependent on CA-induced AhR-*Mta2* recruitment to the *stc2* XREs and played critical role in the regulation of *stc2* gene expression (Joshi et al., 2017). Current study extends from our previous observation and utilize cross-linking chromatin immunoprecipitation coupled mass spectrometry (xChIP-MS) to identify additional histone epigenetic marks namely, TCDD-specific *H3 K14* acetylation, *H3 K23* acetylation and *H3 K27* dimethylation as well as CA-exclusive *H3 K79* methylation at AhR-bound chromatin complex.

In the present study, we demonstrated transient binding of *H4 lysine 5* acetylation and stable association of *H3 lysine 79* methylation (*H3 K79me*) at the AhR-bound *stc2* promoter in response to CA treatment. Moreover, *H4 K5ac* and *H3 K79me*

marks were concurrent with the interaction of histone modification writers Atf2 and Dot1l to the AhR-complex at the *stc2* promoter resulting in target gene induction. Finally, this study has enhanced our understanding of AhR biology by exhibiting that the dynamic quaternary structure of the *stc2* promoter containing XREs encodes comprehensive epigenetic and chromatin structural information necessary for the CA-specific AhR binding and AhR-mediated transcription of *stc2*.

Materials and Methods

Animals, cell culture and treatments. 8 to 10-week-old C57BL/6 (wild-type, WT) (Jackson Laboratories, Bar Harbor, ME) female mice were used in compliance with the guidelines of the Institutional Animal Care and Use Committee (IACUC) at the University of Oklahoma Health Sciences Center (OUHSC) and the University of Texas Medical Branch (UTMB). Mice were treated by oral gavage with vehicle (corn oil), 20 µg/kg 2,3,7,8-tetrachlorodibenzo-p-dioxin (TCDD) (AccuStandard, New Haven, CT) or i.p. injection with 12 mg/kg cinnabarinic acid (CA) (synthesized by Synthetic Organic Chemistry Core at UTMB) for 0, 5, 10, 15, 30 min and 1, 2, 4, 6, 8, 12, 24 hr before sacrifice. For cell culture experiments, AML12 cell-line, a differentiated non-transformed mouse hepatic cells (ATCC, CRL-2254) were plated at a density of 500,000 cells/cm² in DMEM:F12 medium containing 10 µg/ml insulin, 5.5 µg/ml transferrin, 5 ng/ml selenium, 40 ng/ml dexamethasone, penicillin (100 U/ml), streptomycin (100 µg/ml) and 5% fetal bovine serum (FBS). AML12 cells were transiently transfected with ON-TARGETplus Atf2 and Dot1l siRNAs (ThermoFisher Scientific, Waltham, MA) for 24 hr using Metafectene PRO (Biontex Laboratories, GmbH München, Germany) transfection agent. Cells were further treated with 6 nM TCDD, 30 µM CA or vehicle (DMSO) for 2 hr. In both cell culture and animal studies, treatment with vehicle, TCDD and CA were performed blindly to the experimenter by another individual.

Crosslinking chromatin immunoprecipitation coupled LC-targeted MS / MS (xChIP-MS). Upon TCDD or CA treatments, liver tissues from WT mice were extracted, finely minced, and subjected to two-step crosslinking chromatin immunoprecipitation (Tian et al., 2012). Briefly, minced livers were crosslinked using 2 mM disuccinimidyl

glutarate (DSG, 7.7 Å spacer arm) (ThermoFisher Scientific) in phosphate buffered saline for 45 min at room temperature. Further cross-linking with 1% formaldehyde (ThermoFisher Scientific) in phosphate buffered saline was carried out at room temperature for 10 min. Crosslinked samples were homogenized using Dounce homogenizer and centrifuged at 3200 x g for 5 min at 4°C. The supernatant was discarded and the pellet was resuspended in the cell lysis buffer (150 mM NaCl, 25 mM Tris [pH 7.5], 5 mM EDTA, 1% Triton X, 0.1% SDS, 0.5% deoxycholate, protease inhibitor cocktail), Dounce homogenized, incubated on ice for 20 min, centrifuged at 3200 x g for 5 min at 4°C, and the pellet was processed using ChIP-IT Express shearing Kit (Active Motif, Carlsbad, CA). Genomic DNA shearing was performed with adaptive focused acoustic sonicator (Covaris, Woburn, MA) to yield ~ 400 bp DNA fragments bound to protein complex. Immunoprecipitation was carried out by antibody targeting AhR (abcam, Cambridge, MA). Protein-DNA complexes were eluted using elution buffer provided in the kit. Proteins were extracted using SDS loading buffer containing 100 mM DTT followed by incubation at 100°C for 10 min. Proteins were separated using SDS-PAGE gel electrophoresis, stained with Coomassie blue, destained and bands cut out for subsequent mass spectrometry analysis. Gel bands were washed three times with 50% methanol and deionized water, dried by a piece of tissue paper and grinded into fine powder with a tip-sealed 200 µl pipette tip. 50 mM ammonium bicarbonate (100 µl) was added to cover the gel powder. Samples were digested overnight at 37°C by addition of 2 µg trypsin. Digested peptides were extracted by acetonitrile, dried by speedvac and then re-dissolve in 50 µl of 1% formic acid for LC-MS/MS analysis. Peptide mixtures were separated by reversed-phase liquid chromatography using an Easy-nanoLC

equipped with an autosampler (ThermoFisher Scientific). A PicoFrit 25 cm length × 75-
μm id, ProteoPep™ analytical column packed with a mixed (1:1) packing material
(Waters XSelect HSS T3, 5μ , and Waters YMC ODS-AQ, S-5, 100Å) was used to
separate peptides by reversed-phase liquid chromatography (solvent A, 0.1% formic
acid in water; solvent B, 0.1% formic acid in acetonitrile), running with a 176-min of
gradient from 2 to 45% of solvent B with a flow rate at 300 μL/min. The QExactive mass
analyzer (ThermoFisher Scientific GmbH, Bremen, Germany) was set to acquire data at
a resolution of 35,000 in full scan mode and 17,500 in MS/MS mode. The top 15 most
intense ions in each MS survey scan were automatically selected for MS/MS. Peptides
were identified by PEAK® 8.5 (Bioinformatics Solutions, Waterloo, Canada) to perform
De Novo sequencing assisted search against the mouse database (Searched Entry:
52485). Acetylation, mono-methylation, di-methylation, tri-methylation and citrullination
of lysine were set as variable modifications. FDR were estimated by the ratio of decoy #
hits over target # hits among PSMs. Maximum allowed -10logP is >=15.

RNA isolation and quantitative RT-PCR. Total RNA was isolated from vehicle,
TCDD and CA treated mice livers and AML12 cells using Trizol (ThermoFisher
Scientific). cDNA was prepared from 1 μg total RNA using iScript cDNA synthesis kit
(Bio-Rad, Hercules, California). Quantitative RT-PCR was performed using
StepOnePlus real time PCR system (ThermoFisher Scientific) using cyp1a1 Forward 5'
GCCTAACTCTTCCCTGGATGC 3', cyp1a1 Reverse 5'
TCAATGAGGCTGTCTGTGATGTC 3', stc2 Forward 5'
GTCGGTGTGATTGTGGAGATGAT, stc2 Reverse 5' TCCACATAGGGCTCATGCAG,
18s rRNA Forward 5' CTCAACACGGGAAACCTCAC 3' and 18s rRNA reverse 5'

CGCTCCACCAACTAAGAACG 3' primers and PowerUp SYBR Green Master Mix (ThermoFisher Scientific).

Chromatin Immunoprecipitation (ChIP). Following treatments with vehicle, TCDD and CA, liver tissues from WT mice were extracted, finely minced and fixed with 1% formaldehyde in phosphate buffered saline at room temperature for 10 min. Livers were homogenized using Dounce homogenizer, centrifuged at 3200 x g for 5 min at 4°C, and resuspended in 2 ml cell lysis buffer (150 mM NaCl, 25 mM Tris [pH 7.5], 5 mM EDTA, 1% Triton X, 0.1% SDS, 0.5% deoxycholate, protease inhibitor cocktail). Samples were incubated on ice for 15 min, centrifuged at 3200 x g for 5 min at 4°C and processed through ChIP-IT Express Enzymatic Kit (Active Motif) according to manufacturer's instructions. AML12 cells were crosslinked with 1% formaldehyde and processed as per the manufacturer's protocol (Active Motif). Antibodies against AhR, histone H3 (ab cam); histone H4, histone H4 K5ac, histone H3 K79me, IgG (Cell Signaling Technology, Danvers, MA); Atf2, Dot1l (Santacruz Biotechnology, Dallas) were used to immunoprecipitate protein bound DNA complexes. Immunoprecipitated and input DNA was PCR amplified using primers specific to the cyp1a1 and stc2 promoters flanking the XREs. The cyp1a1 and stc2 PCR primer pairs are cyp1a1 forward 5'-CTATCTCTTAAACCCACCCCAA-3', cyp1a1 reverse 5'-CTAAGTATGGTGGAGGAAAGGGTG-3' and stc2 forward 5'-CTCAGTCCATTGGGCCATTGCCC-3', stc2 reverse 5'-AGGAAGCGGAGCGCCTCCGC-3'. For ChIP assays performed on the CRISPR/Cas9 edited AML12 cells cyp1a1 forward 5' CAGGGGAGGGCAGGTGAAGG 3' and cyp1a1 reverse 5' TGGTGACTTTGCTTCCCTGG 3' primers were used. PCR products were

fractionated on a 5% polyacrylamide gel, stained with SYBR Green (ThermoFischer Scientific) and imaged on a ChemiDoc MP imaging system (Bio-Rad).

xChIP-Western blotting and Western blotting. Two-step crosslinking chromatin immunoprecipitation (xChIP) using anti-AhR antibody was performed as described in the aforementioned xChIP-MS protocol. Upon crosslinking and chromatin immunoprecipitation using anti-AhR antibody, proteins were extracted with SDS loading buffer containing 100 mM DTT followed by incubation at 100°C for 10 min. Protein samples were fractionated by SDS-PAGE using Mini-Protean electrophoresis system (Bio-Rad) and transferred to 0.45 µm LF PVDF membranes (Bio-Rad) using Trans-blot turbo system (Bio-Rad). Membranes were probed with antibodies against histone H4, H4 K5ac, H3 K79me, H3 K14ac, H3 K23ac, H3 K27dime, p300, Cbp (Cell Signaling Technology); Atf2, Dot1l, Tip60, Mta2 (Santacruz Biotechnology); histone H3 (ab cam). For AML12 cells, extracts were prepared using cell lysis buffer (Cell Signaling Technology) and upon Western blotting were probed with anti-Atf2, anti-Dot1l (Santacruz Biotechnology), and anti-actin (Millipore Sigma, Sr Louis, MO) antibodies. Proteins were detected using IRDye 800CW and IRDye 680RD secondary antibodies (Li-COR, Lincoln, Nebraska) followed by imaging using an Odyssey CLx imaging system (Li-COR).

Replacement of cyp1a1 promoter XREs with 'stc2 XRE cassette' in AML12 cells. Using CRISPR-Cas9 editing, modified AML12 cell line was constructed by replacing 926 bp cyp1a1 promoter region (between -574 and -1500 from transcription start site) containing 10 XREs with 259 bp stc2 promoter region (- 210 to - 469) encompassing 8 XREs – 'stc2 XRE cassette' (Supp. Fig. 1A). Using Universal CRISPR activity assay

(Biocytogen, Wakefield, MA) TCTGGGCTCGGGAGCTCACA GGG as 5' sgRNA and GGCACCCATTGGCTTGTAGT AGG as 3' guide sgRNA were chosen. Target vector construction, electroporation, and screening of positive clones was performed (Biocytogen). Junction PCR using HR allele primer pairs: CL-JGY-002-A-L-GT-F (TGTAAGGGTCGGGTGTCCTGAGAAT), Puromycin-GT-F (GCAACAGATGGAAGGCCTCCTGGCG) and CL-JGY-002-A-R-GT-F (GCGGTCCTTCGGGCACCTCGAC), CL-JGY-002-A-R-GT-R (TGGTGTTTCCAGTTCCTGAAGCTC), non-HR allele primers CL-JGY-002-A-R-GT-F1 (GTTGTAAACTGTCCCCTGCATATC) and CL-JGY-002-A-R-GT-R (TGGTGTTTCCAGTTCCTGAAGCTC) as well as DNA sequencing confirmed successful donor vector integration. A homozygous clone D02 was used in the present studies (referred to as CRISPR/Cas9 edited AML12 cells) (Supp. Fig. 1).

Statistical Analysis. xChIP-MS and xChIP-Western blotting assays to identify TCDD and CA-specific histone modifications and modifiers respectively were exploratory in nature. The xChIP-Western blotting (to confirm newly identified histone modifications), ChIP and qRT-PCR experiments were conducted with a preset plan. The sample sizes per group, blinding and data analysis methodology were predetermined (Michel et al., 2020). Data were analyzed by applying analysis of variance (ANOVA) models using Sigma Stat software (Systat Software, San Jose, CA). Differences between the groups were considered significant only if the *p* value is < 0.05.

Results

CA and TCDD induced differential gene expression of stc2 and cyp1a1. We have previously assessed mutually exclusive expression of AhR target genes, cyp1a1 and stc2 in response to 2 hr TCDD and CA treatments (Joshi et al., 2015; Joshi et al., 2017). Here, we measured cyp1a1 and stc2 mRNA message in the livers of TCDD (20 µg/kg) and CA (12 mg/kg) treated WT mice at different time points (Fig. 1). TCDD-driven induction of cyp1a1 was observed at 5 min and is plateaued at 1 hr (Fig. 1A). Maximal stc2 induction by CA was achieved at 24 hr with significant reduction in the message at 48 hr (Fig. 1B). Vehicle treatment did not elicit cyp1a1 or stc2 induction (Supp. Fig. 2A). The data confirmed that the agonist-specific dichotomous expression of cyp1a1 and stc2 persists temporally.

Identification of CA and TCDD specific histone post-translational modifications. To evaluate involvement of distinct epigenetic modifications in agonist-specific differential gene regulation, CA and TCDD-treated livers were crosslinked with protein-protein and protein-DNA crosslinkers and subjected to chromatin immunoprecipitation using anti-AhR antibody followed by mass spectrometry (xChIP-MS) (Sowers et al., 2015; Tian et al., 2012). xChIP-MS identified TCDD-specific histone H3 lysine 14 acetylation (H3 K14ac), lysine 23 acetylation (H3 K23ac), lysine 27 dimethylation (H3 K27dime) and CA-specific stable H3 K79 methylation (H3 K79me) marks at the AhR-bound chromatin complex (Fig. 2A and B). Moreover, we have previously confirmed association of H4 K5 acetylation (H4 K5ac) at AhR-bound stc2 promoter after CA but not upon TCDD or vehicle treatments (Fig. 2A) (Joshi et al., 2017). To verify interaction of specific epigenetic marks within AhR-bound chromatin, Western blotting on

crosslinked chromatin immunoaffinity purified AhR complexes (xChIP-WB) was performed. TCDD-specific association of AhR-complex with H3 K14ac at 48 hr; H3 K23ac at 4, 6, 8, 12 and 48 hr; and H3 K27dime between 2 to 48 hr was validated (Fig. 3). Histone H3 K14ac, K23ac and K27dime marks were not observed at AhR-bound chromatin upon CA or vehicle treatments (Fig. 3 and Supp. Fig. 2B). CA-specific AhR-bound H4 K5ac expression was transient between 2 to 24 hr – contemporaneous with CA-induced *stc2* expression (Fig. 3). xChIP-immunoblotting also confirmed stable interaction of H3 K79me with CA-induced AhR complex (Fig. 3).

Chromatin regulators associated with AhR-bound chromatin complex. Given that the histone post-translational modifications are vital for regulating chromatin architecture and dynamic homeostasis of these modifications are driven by the recruitment of chromatin regulators such as ‘writers’ of histone modifications (Gillette and Hill, 2015), we sought to identify AhR-bound regulators of CA-specific histone modifications. We focused on specific histone modification ‘writers’ that are known or are likely to trigger H4 K5 acetylation and H3 K79 methylation (Hyun et al., 2017; Marmorstein and Zhou, 2014; Sandoval et al., 2016). xChIP-Western blotting revealed CA-specific interaction of known H4 K5 acetylation writer – activating transcription factor 2 (Atf2) with AhR-chromatin complex between 2 and 24 hr, concurrent with H4 K5 acetylation and *stc2* induction (Fig. 4 and Supp. Fig. 2C). We were able to recapitulate previously detected association of histone reader, Mta2 with AhR uniquely in response to CA treatment (Joshi et al., 2017). Furthermore, CA-treatment resulted in an interaction of AhR-bound chromatin complex with a known H3 K79 methylation writer, disruptor of telomeric silencing 1-like histone lysine methyltransferase (Dot1l) (Fig. 4). Other lysine

acetyltransferases examined including p300, Cbp and Tip60 were associated with AhR-chromatin complex in response to both TCDD and CA treatments but not upon administration of the vehicle (Fig. 4 and Supp. Fig 2C).

CA-specific direct recruitment of chromatin modification writers to stc2 promoter in vivo. The 218 bp region of stc2 promoter between -244 and -462 bp upstream of transcription start site contain 8 distinct XREs (Harper et al., 2013). Prior studies have demonstrated recruitment of AhR-Arnt-Mta2 complex to stc2 promoter sequence in response to CA treatment (Joshi et al., 2015; Joshi et al., 2017). Here, we examined whether histone H4 K5 acetylation and H3 K79 methylation writers, Atf2 and Dot1l were recruited to the stc2 promoter encompassing the XRE cluster. Chromatin immunoprecipitation assay was performed on whole-liver tissue targeting XREs within stc2 and cyp1a1 promoter regions. CA-specific recruitment of Atf2 to stc2 promoter was observed between 2 and 24 hr, concurrent with the AhR binding (Fig. 5), H4 K5 acetylation (Fig. 3) and elevated stc2 expression (Fig. 1). Dot1l was stably bound to the stc2 promoter upon CA treatment (Fig. 5). Neither Atf2 and Dot1l were recruited to the cyp1a1 promoter upon CA treatment nor to the stc2 and cyp1a1 XREs upon TCDD or vehicle administration (Fig. 5 and Supp. Fig. 2D). Finally, AhR was bound directly to the cyp1a1 promoter upon TCDD treatment inducing cyp1a1 expression (Fig. 5).

Histone writers Atf2 and Dot1l are essential for CA-driven stc2 expression. AML12 cells were transiently transfected with Atf2, Dot1l and Non-Targeting (scrambled) siRNA oligonucleotides. Western blotting confirmed successful knock-down of Atf2 and Dot1l protein expression with RNA interference (Fig. 6A). Quantitative RT-PCR indicated that the loss of Atf2 and Dot1l significantly attenuated CA-induced stc2

expression whereas the *cyp1a1* message remained unaltered (Fig. 6B). ChIP studies revealed that silencing *Atf2* obliterated AhR recruitment to *stc2* promoter and impeded H4 K5 acetylation (Fig. 6C). Similarly, suppressing *Dot1l* expression resulted in the loss of AhR and H4 K79me interaction at *stc2* promoter. Silencing histone modification writers had no effect on TCDD-driven AhR binding to *cyp1a1* promoter (Fig. 6C). Collectively, our data suggests that the CA-driven recruitment of chromatin regulators, *Atf2* and *Dot1l* to AhR-chromatin complex triggers histone epigenetic modifications, including histone H4 K5 acetylation and H3 K79 methylation exclusively at *stc2* promoter plausibly resulting in changes in chromatin structure thereby inducing *stc2* expression.

Role of quaternary XRE structure in agonist-specific differential gene regulation.

We examined whether the quaternary structure of the *stc2* promoter encompasses complete epigenetic and structural information necessary for the agonist specific recruitment of chromatin regulators, histone modifications and AhR-mediated regulation of *stc2*. A modified AML12 cell line was constructed by replacing 926 bp *cyp1a1* promoter region containing 10 XREs (between -574 and -1500 bp from transcription start site) with *stc2* promoter containing 8 XREs (between -210 to -469 bp from transcription start site, termed 'stc2 XRE cassette') using CRISPR/Cas9 editing (Fig. 7A). In the CRISPR/Cas9 edited AML12 cells, quantitative RT-PCR indicated upregulation of *cyp1a1* gene expression in response to CA treatment (Fig. 7B). A marked reduction in *cyp1a1* message upon TCDD treatment in edited cells was attributed to the lack of 10 XREs within *cyp1a1* promoter (Fig. 7B). ChIP studies performed in WT AML12 cells displayed direct binding of AhR to *cyp1a1* promoter upon

TCDD treatment (Fig. 7C). In CRISPR/Cas9 edited AML12 cells – AhR, Atf2 and Dot1l binding as well as interaction of H4 K5 acetylation and H3 K79 methylation to 'stc2 XRE cassette' within cyp1a1 promoter was observed exclusively in response to CA treatment (Fig. 7C). These results strongly suggest that the agonist-specific AhR-mediated stc2 expression can be transferred with the stc2 promoter sequence in the context of chromatin architecture. Finally, this study confirmed that the quaternary DNA structure contain comprehensive epigenetic and higher-order chromatin conformational information necessary to elucidate agonist-specific differential gene regulation by AhR.

Discussion

Since its discovery in 1976, Aryl hydrocarbon receptor has been a pivotal transcription factor in both environmental toxicology and molecular pharmacology (Poland et al., 1976a; Poland et al., 1976b). Apart from the identification of prototypical AhR ligands of anthropic origin, over the last 40 years number of natural structurally diverse AhR ligands with varying binding affinities have been discovered (Denison and Nagy, 2003; Denison et al., 2011). Moreover, a recent identification of the endogenous AhR agonist, CA presents a unique opportunity to study molecular mechanism underlying the CA and TCDD specific mutually exclusive regulation of *stc2* and *cyp1a1* genes by AhR (Harper et al., 2013; Joshi et al., 2015; Lowe et al., 2014). Our previous studies using electrophoretic mobility shift assays (EMSA) showed AhR binding to radiolabeled oligonucleotide probes encompassing individual *cyp1a1* and *stc2* promoter XREs in response to both TCDD and CA treatments (Joshi et al., 2017). This observation suggested that the agonist-specific AhR-mediated differential transcription regulation was ‘at least in part’ dependent on the tertiary chromatin structure plausibly due to the distinct cofactor binding and specific epigenetic modifications. Very few studies have reported evidence of ligand-specific cofactor recruitment by AhR. In mammalian cell culture systems, ligand-selective interaction of AhR with several cofactors including SRC1, SRC2, STC3, TRAP220, CARM1, and PGC1 was observed using two-hybrid assays (Zhang et al., 2008). Moreover, AhR agonists β -naphthoflavone and 3,3'-diindolylmethane (DIM) displayed differential cofactor recruitment to the *cyp1a1* promoter in MCF7 cells (Hestermann and Brown, 2003). Agonist-specific cofactor binding was also observed in other nuclear receptors including glucocorticoid receptor

(Monczor et al., 2019), androgen receptor (Muller et al., 2000), and epidermal growth factor receptor (ErbB/HER) (Saeki et al., 2009). However, the findings presented here are unique as our results indicate CA-specific recruitment of distinct histone modification writers (Atf2 and Dot1l) to AhR-chromatin complex, resulting in specific epigenetic modifications (H4 K5ac, H3 K79me) at *stc2* promoter *in vivo*, responsible for regulating transcription of *stc2*.

Gene transcription is a highly orchestrated process tightly regulated by the local chromatin conformation (Chen and Li, 2010; Woodcock and Ghosh, 2010). The basic unit of chromatin, the nucleosome core contains two copies of four types of histones (H2A, H2B, H3 and H4) that can be post-translationally altered into at least 80 known covalent modifications (Zhao and Garcia, 2015). These histone modifications produce ‘histone code’ that influence nucleosome compactness and chromatin organization resulting in activation or silencing of transcription (Bannister and Kouzarides, 2011; Bartke and Kouzarides, 2011; Kouzarides, 2007). Our previous mass spectrometry analysis performed on the liver nuclei isolated from TCDD and CA treated mice identified CA-specific H4 K5 acetylation (Joshi et al., 2017). Further studies confirmed that the H4 K5ac at the *stc2* promoter was concomitant with the interaction of Mta2 – a known chromatin modification ‘reader’ – with the AhR (Joshi et al., 2017). In order to catalog CA and TCDD specific histone modifications associated with AhR-bound chromatin temporally, we performed crosslinking chromatin immunoprecipitation coupled to LC-MS/MS (xChIP-MS) (Sowers et al., 2015; Tang et al., 2016; Tian et al., 2012). A parallel reaction monitoring, an ion monitoring technique based on high-resolution high-precision mass spectrometry was employed to simultaneously detect

multiple histone modifications. Parallel reaction monitoring has a broad dynamic range, measures all transitions, and is more resistant to background noise than conventional selective reaction monitoring (Tang et al., 2014). xChIP-MS identified a myriad of AhR-bound stable and transient histone acetylations and methylations across genome, albeit we focused on CA and TCDD specific mutually exclusive modifications. Histone H3 K14 acetylation, H3 K23 acetylation and H3 K27 dimethylation were uniquely observed at AhR-bound chromatin in response to TCDD treatment. Whereas, CA triggered stable association of H3 K79 methylation at AhR-chromatin complex (Fig. 2). Surprisingly, we did not detect H4 K5 acetylation with high confidence possibly due to the limitation of signal detection by MS, low abundance or loss during sample preparation (Bensaddek and Lamond, 2016). Nevertheless, xChIP-Western blotting successfully confirmed presence of H4 K5ac at AhR-bound chromatin exclusively upon CA treatment (Fig. 3).

Modifications on histone H4, specifically lysine residues in N-terminal tail (K5, 8, 12 and 16), are known to be involved in gene regulation and maintaining genome integrity (Shahbazian and Grunstein, 2007; Turner et al., 1989; Zheng et al., 2013). H4 K5 has largely been implicated in epigenetic priming (Park et al., 2013), bookmarking (Zhao et al., 2011) as well as transcription regulation (Borsos et al., 2015). Histone acetylation is controlled by families of non-redundant lysine acetyltransferase (KATs), which use acetyl CoA to form ϵ -N-acetyllysine on lysine residues of histone tails, neutralizes the positive charge on histone lysines, decreases the DNA-histone interaction, opens the chromatin structure, and facilitates recruitment of RNA polymerase II resulting in transcription activation of target genes (Bartke and Kouzarides, 2011). Previous studies have identified and characterized Tip60, Hbo1

(Myst2), Cbp, p300, and Atf2 as known H4 K5 acetylation writers (Legube and Trouche, 2003). Moreover, several chromatin regulators are known to interact with AhR, including p300, Cbp, Src1, Tif2, p/CIP (Beischlag et al., 2002; Kobayashi et al., 1997). In this study, we reiterated interaction of histone acetylation ‘writers’ – p300, Cbp and Tip60 to AhR irrespective of agonist specificity (Fig. 4). On the contrary, Atf2 was associated with AhR-stc2 promoter complex exclusively in response to CA treatment. Atf2 is a member of the ATF/cAMP response element binding (CREB) protein family of basic region leucine zipper proteins and a bona-fide candidate reported to possess intrinsic lysine acetyltransferase activity (Nomura et al., 1993; Sheikh and Akhtar, 2019). Atf2 is known to interact with other transcription factors as well as bind to response elements on target genes and stimulate distinct transcription programs. Association of Atf2 with AP1 is known to alter local DNA structure and initiate transcription, Atf2-Jun interaction mediate transcription of IFN β , and Atf2 binding to β HLH-PAS family member – HIF1 α promotes its transcription activity (Choi et al., 2009; Falvo et al., 2000; Falvo et al., 1995). Therefore, it is conceivable that CA-specific interaction of Atf2 with AhR can directly or by recruitment of additional lysine acetyltransferases acetylate histone H4 K5. The acetylated mark is then accessed by chromatin modification readers such as previously identified Mta2 (Joshi et al., 2017; Wu, 2013) and/or Brd4 which employs the bromodomain to target the modified histone and regulate transcription (Shi and Vakoc, 2014).

This study also identified CA-specific stable association of H3 K79methylation at the AhR-chromatin complex (Fig. 2 and 3). Histone H3 K4methylation, K36methylation, and K79methylation are the three histone H3 methylation marks known to be associated

with an active form of chromatin (Hyun et al., 2017). ChIP-Chip arrays using H3 K79 methylation antibodies have revealed positive correlation of gene expression in mammalian cells with the recruitment of histone methyltransferase, Dot1l (Steger et al., 2008). Therefore, it is plausible that the CA-driven AhR-mediated recruitment of histone modification ‘writers’ – Atf2 and Dot1l confer specific epigenetic marks including H4 K5ac and H3 K79me, remodel the chromatin structure and provide access to the transcription machinery at the *stc2* promoter. It is noteworthy, that AhR and Atf2 recruitment to the *stc2* promoter and H4 K5 acetylation correlates with the kinetics of the *stc2* induction. However, binding of Dot1l and H3 K79 methylation occurs as early as 5 minutes post CA treatment (Fig. 1 to 5). Previous studies have noted kinetic discrepancies between binding of AhR, p300, Src1, Tif2, p/CIP to the *cyp1a1* promoter and *cyp1a1* gene expression in response to different ligands (Hestermann and Brown, 2003). It is therefore feasible that additional transcription factors, coregulators and signaling pathways including pRb, E2F, RelA, NF-κB, estrogen receptor, Nrf2/Maf might cross-talk with CA and/or CA-bound AhR and thereby influence *stc2* regulation (Denison et al., 2011; Jackson et al., 2014). Further chromatin proteomic profiling (David et al., 2017) as well as ChIP-seq studies are warranted to address differences in the kinetics and its impact on the agonist specific AhR-mediated gene regulation.

A modified AML12 cell line was constructed by replacing known dioxin-responsive elements within *cyp1a1* promoter with the *stc2* cassette containing 8 XREs (Lusska et al., 1993; Shen et al., 1991). In the CRISPR/Cas9 edited AML12 cells, histone epigenetic modifications (H4 K5ac, H3 K79me) and chromatin modification ‘writers’ (Atf2, Dot1l) were transferred in conjunction with the quaternary structure of the

stc2 promoter XREs resulting in a CA-dependent regulation of cyp1a1 expression. This reinforced the notion that the agonist-specific gene regulation by AhR is highly dependent on the ligand-specific cofactor recruitment and exclusive epigenetic signatures that influence chromatin architecture (Wajda et al., 2020). The diminished but persistent induction of cyp1a1 by TCDD in the edited cells is attributed to the functional XREs located beyond -1500 bp from transcription start site as acknowledged in the ChIP-seq studies (Fig. 7) (Nault et al., 2016). Our future studies beyond the scope of this manuscript will reveal genome-wide chromatin accessibility and nucleosome occupancy in response to CA versus TCDD treatments, determine presence of the CA-specific epigenetic signatures at other AhR-target genes, identify molecular interactions of AhR with the 'readers' and 'erasers' of histone modifications, and will ultimately probe into the mechanics of chromatin remodeling in response to the AhR agonists. Collectively, these observations strongly demonstrate that the distinct cofactor binding and epigenetic modifications play critical role in the agonist specific AhR mediated gene expression and highlights the complexities involved in the transcription regulation by AhR.

Acknowledgements

We thank Dr. Cornelis Elferink (University of Texas Medical Branch, Galveston) for the helpful discussions regarding xChIP-MS data analysis and CRISPR/Cas9 studies.

Authorship Contributions

Participated in research design: Joshi

Conducted experiments: Patil, Tang, Rus, Joshi

Contributed new reagent or analytical tools: Patil, Tang, Rus, Zhang, Joshi

Performed data analysis: Patil, Tang, Zhang, Joshi

Wrote or contributed to the writing of the manuscript: Patil, Tang, Zhang, Joshi

References

- Bannister AJ and Kouzarides T (2011) Regulation of chromatin by histone modifications. *Cell research* 21(3): 381-395.
- Bartke T and Kouzarides T (2011) Decoding the chromatin modification landscape. *Cell Cycle* 10(2): 182.
- Beischlag TV, Wang S, Rose DW, Torchia J, Reisz-Porszasz S, Muhammad K, Nelson WE, Probst MR, Rosenfeld MG and Hankinson O (2002) Recruitment of the NCoA/SRC-1/p160 family of transcriptional coactivators by the aryl hydrocarbon receptor/aryl hydrocarbon receptor nuclear translocator complex. *Molecular and cellular biology* 22(12): 4319-4333.
- Bensaddek D and Lamond AI (2016) Unlocking the chromatin code by deciphering protein-DNA interactions. *Mol Syst Biol* 12(11): 887.
- Borsos BN, Pankotai T, Kovacs D, Popescu C, Pahi Z and Boros IM (2015) Acetylations of Ftz-F1 and histone H4K5 are required for the fine-tuning of ecdysone biosynthesis during *Drosophila* metamorphosis. *Dev Biol* 404(1): 80-87.
- Chen P and Li G (2010) Dynamics of the higher-order structure of chromatin. *Protein Cell* 1(11): 967-971.
- Choi JH, Cho HK, Choi YH and Cheong J (2009) Activating transcription factor 2 increases transactivation and protein stability of hypoxia-inducible factor 1alpha in hepatocytes. *The Biochemical journal* 424(2): 285-296.

David SA, Piegu B, Hennequet-Antier C, Pannetier M, Aguirre-Lavin T, Crochet S, Bordeau T, Courousse N, Brionne A, Bigot Y, Collin A and Coustham V (2017) An Assessment of Fixed and Native Chromatin Preparation Methods to Study Histone Post-Translational Modifications at a Whole Genome Scale in Skeletal Muscle Tissue. *Biol Proced Online* 19: 10.

Denison MS and Nagy SR (2003) Activation of the aryl hydrocarbon receptor by structurally diverse exogenous and endogenous chemicals. *Annual review of pharmacology and toxicology* 43: 309-334.

Denison MS, Soshilov AA, He G, DeGroot DE and Zhao B (2011) Exactly the same but different: promiscuity and diversity in the molecular mechanisms of action of the aryl hydrocarbon (dioxin) receptor. *Toxicological sciences : an official journal of the Society of Toxicology* 124(1): 1-22.

Elferink CJ, Gasiewicz TA and Whitlock JP, Jr. (1990) Protein-DNA interactions at a dioxin-responsive enhancer. Evidence that the transformed Ah receptor is heteromeric. *The Journal of biological chemistry* 265(33): 20708-20712.

Elferink CJ and Whitlock JP, Jr. (1990) 2,3,7,8-Tetrachlorodibenzo-p-dioxin-inducible, Ah receptor-mediated bending of enhancer DNA. *The Journal of biological chemistry* 265(10): 5718-5721.

Falvo JV, Parekh BS, Lin CH, Fraenkel E and Maniatis T (2000) Assembly of a functional beta interferon enhanceosome is dependent on ATF-2-c-jun heterodimer orientation. *Molecular and cellular biology* 20(13): 4814-4825.

Falvo JV, Thanos D and Maniatis T (1995) Reversal of intrinsic DNA bends in the IFN beta gene enhancer by transcription factors and the architectural protein HMG I(Y). *Cell* 83(7): 1101-1111.

Flaveny CA, Murray IA and Perdew GH (2010) Differential gene regulation by the human and mouse aryl hydrocarbon receptor. *Toxicological sciences : an official journal of the Society of Toxicology* 114(2): 217-225.

Fukunaga BN, Probst MR, Reisz-Porszasz S and Hankinson O (1995) Identification of functional domains of the aryl hydrocarbon receptor. *The Journal of biological chemistry* 270(49): 29270-29278.

Gillette TG and Hill JA (2015) Readers, writers, and erasers: chromatin as the whiteboard of heart disease. *Circulation research* 116(7): 1245-1253.

Hankinson O (1993) Research on the aryl hydrocarbon (dioxin) receptor is primed to take off. *Archives of biochemistry and biophysics* 300(1): 1-5.

Hankinson O (1995) The aryl hydrocarbon receptor complex. *Annual review of pharmacology and toxicology* 35: 307-340.

Harper TA, Jr., Joshi AD and Elferink CJ (2013) Identification of stanniocalcin 2 as a novel aryl hydrocarbon receptor target gene. *The Journal of pharmacology and experimental therapeutics* 344(3): 579-588.

Hestermann EV and Brown M (2003) Agonist and chemopreventative ligands induce differential transcriptional cofactor recruitment by aryl hydrocarbon receptor. *Molecular and cellular biology* 23(21): 7920-7925.

Hubbard TD, Murray IA and Perdew GH (2015) Indole and Tryptophan Metabolism: Endogenous and Dietary Routes to Ah Receptor Activation. *Drug Metab Dispos* 43(10): 1522-1535.

Hyun K, Jeon J, Park K and Kim J (2017) Writing, erasing and reading histone lysine methylations. *Exp Mol Med* 49(4): e324.

Jackson DP, Li H, Mitchell KA, Joshi AD and Elferink CJ (2014) Ah receptor-mediated suppression of liver regeneration through NC-XRE-driven p21Cip1 expression. *Molecular pharmacology* 85(4): 533-541.

Jones PB, Durrin LK, Fisher JM and Whitlock JP, Jr. (1986) Control of gene expression by 2,3,7,8-tetrachlorodibenzo-p-dioxin. Multiple dioxin-responsive domains 5'-ward of the cytochrome P1-450 gene. *The Journal of biological chemistry* 261(15): 6647-6650.

Joshi AD, Carter DE, Harper TA, Jr. and Elferink CJ (2015) Aryl hydrocarbon receptor-dependent stanniocalcin 2 induction by cinnabarinic acid provides cytoprotection against endoplasmic reticulum and oxidative stress. *The Journal of pharmacology and experimental therapeutics* 353(1): 201-212.

Joshi AD, Hossain E and Elferink CJ (2017) Epigenetic Regulation by Agonist-Specific Aryl Hydrocarbon Receptor Recruitment of Metastasis-Associated Protein 2 Selectively Induces Stanniocalcin 2 Expression. *Molecular pharmacology* 92(3): 366-374.

Kobayashi A, Numayama-Tsuruta K, Sogawa K and Fujii-Kuriyama Y (1997) CBP/p300 functions as a possible transcriptional coactivator of Ah receptor nuclear translocator (Arnt). *J Biochem* 122(4): 703-710.

- Kouzarides T (2007) Chromatin modifications and their function. *Cell* 128(4): 693-705.
- Legraverend C, Hannah RR, Eisen HJ, Owens IS, Nebert DW and Hankinson O (1982) Regulatory gene product of the Ah locus. Characterization of receptor mutants among mouse hepatoma clones. *The Journal of biological chemistry* 257(11): 6402-6407.
- Legube G and Trouche D (2003) Regulating histone acetyltransferases and deacetylases. *EMBO Rep* 4(10): 944-947.
- Lowe MM, Mold JE, Kanwar B, Huang Y, Louie A, Pollastri MP, Wang C, Patel G, Franks DG, Schlezinger J, Sherr DH, Silverstone AE, Hahn ME and McCune JM (2014) Identification of cinnabarinic acid as a novel endogenous aryl hydrocarbon receptor ligand that drives IL-22 production. *PloS one* 9(2): e87877.
- Lusska A, Shen E and Whitlock JP, Jr. (1993) Protein-DNA interactions at a dioxin-responsive enhancer. Analysis of six bona fide DNA-binding sites for the liganded Ah receptor. *The Journal of biological chemistry* 268(9): 6575-6580.
- Ma C, Marlowe JL and Puga A (2009) The aryl hydrocarbon receptor at the crossroads of multiple signaling pathways. *EXS* 99: 231-257.
- Marmorstein R and Zhou MM (2014) Writers and readers of histone acetylation: structure, mechanism, and inhibition. *Cold Spring Harb Perspect Biol* 6(7): a018762.
- McIntosh BE, Hogenesch JB and Bradfield CA (2010) Mammalian Per-Arnt-Sim proteins in environmental adaptation. *Annual review of physiology* 72: 625-645.

Michel MC, Murphy TJ and Motulsky HJ (2020) New Author Guidelines for Displaying Data and Reporting Data Analysis and Statistical Methods in Experimental Biology. *Molecular pharmacology* 97(1): 49-60.

Monczor F, Chatzopoulou A, Zappia CD, Houtman R, Meijer OC and Fitzsimons CP (2019) A Model of Glucocorticoid Receptor Interaction With Coregulators Predicts Transcriptional Regulation of Target Genes. *Front Pharmacol* 10: 214.

Muller JM, Isele U, Metzger E, Rempel A, Moser M, Pscherer A, Breyer T, Holubarsch C, Buettner R and Schule R (2000) FHL2, a novel tissue-specific coactivator of the androgen receptor. *The EMBO journal* 19(3): 359-369.

Nault R, Fader KA, Kirby MP, Ahmed S, Matthews J, Jones AD, Lunt SY and Zacharewski TR (2016) Pyruvate Kinase Isoform Switching and Hepatic Metabolic Reprogramming by the Environmental Contaminant 2,3,7,8-Tetrachlorodibenzo-p-Dioxin. *Toxicological sciences : an official journal of the Society of Toxicology* 149(2): 358-371.

Nebert DW and Gelboin HV (1968a) Substrate-inducible microsomal aryl hydroxylase in mammalian cell culture. I. Assay and properties of induced enzyme. *The Journal of biological chemistry* 243(23): 6242-6249.

Nebert DW and Gelboin HV (1968b) Substrate-inducible microsomal aryl hydroxylase in mammalian cell culture. II. Cellular responses during enzyme induction. *The Journal of biological chemistry* 243(23): 6250-6261.

Nebert DW, Puga A and Vasiliou V (1993) Role of the Ah receptor and the dioxin-inducible [Ah] gene battery in toxicity, cancer, and signal transduction. *Annals of the New York Academy of Sciences* 685: 624-640.

Nguyen LP and Bradfield CA (2008) The search for endogenous activators of the aryl hydrocarbon receptor. *Chemical research in toxicology* 21(1): 102-116.

Nomura N, Zu YL, Maekawa T, Tabata S, Akiyama T and Ishii S (1993) Isolation and characterization of a novel member of the gene family encoding the cAMP response element-binding protein CRE-BP1. *The Journal of biological chemistry* 268(6): 4259-4266.

Park CS, Rehrauer H and Mansuy IM (2013) Genome-wide analysis of H4K5 acetylation associated with fear memory in mice. *BMC genomics* 14: 539.

Poland A, Clover E, Kende AS, DeCamp M and Giandomenico CM (1976a) 3,4,3',4'-Tetrachloro azoxybenzene and azobenzene: potent inducers of aryl hydrocarbon hydroxylase. *Science* 194(4265): 627-630.

Poland A, Glover E and Kende AS (1976b) Stereospecific, high affinity binding of 2,3,7,8-tetrachlorodibenzo-p-dioxin by hepatic cytosol. Evidence that the binding species is receptor for induction of aryl hydrocarbon hydroxylase. *The Journal of biological chemistry* 251(16): 4936-4946.

Saeki Y, Endo T, Ide K, Nagashima T, Yumoto N, Toyoda T, Suzuki H, Hayashizaki Y, Sakaki Y and Okada-Hatakeyama M (2009) Ligand-specific sequential regulation of transcription factors for differentiation of MCF-7 cells. *BMC genomics* 10: 545.

Sandoval J, Pereda J, Perez S, Finamor I, Vallet-Sanchez A, Rodriguez JL, Franco L, Sastre J and Lopez-Rodas G (2016) Epigenetic Regulation of Early- and Late-Response Genes in Acute Pancreatitis. *J Immunol* 197(10): 4137-4150.

Shahbazian MD and Grunstein M (2007) Functions of site-specific histone acetylation and deacetylation. *Annu Rev Biochem* 76: 75-100.

Sheikh BN and Akhtar A (2019) The many lives of KATs - detectors, integrators and modulators of the cellular environment. *Nat Rev Genet* 20(1): 7-23.

Shen ES, Elferink CJ and Whitlock JP, Jr. (1991) Use of gel retardation to analyze protein-DNA interactions upstream of CYP1A1 gene. *Methods in enzymology* 206: 403-408.

Shi J and Vakoc CR (2014) The mechanisms behind the therapeutic activity of BET bromodomain inhibition. *Molecular cell* 54(5): 728-736.

Sowers JL, Mirfattah B, Xu P, Tang H, Park IY, Walker C, Wu P, Laezza F, Sowers LC and Zhang K (2015) Quantification of histone modifications by parallel-reaction monitoring: a method validation. *Analytical chemistry* 87(19): 10006-10014.

Steger DJ, Lefterova MI, Ying L, Stonestrom AJ, Schupp M, Zhuo D, Vakoc AL, Kim JE, Chen J, Lazar MA, Blobel GA and Vakoc CR (2008) DOT1L/KMT4 recruitment and H3K79 methylation are ubiquitously coupled with gene transcription in mammalian cells. *Molecular and cellular biology* 28(8): 2825-2839.

Tang H, Fang H, Yin E, Brasier AR, Sowers LC and Zhang K (2014) Multiplexed parallel reaction monitoring targeting histone modifications on the QExactive mass spectrometer. *Analytical chemistry* 86(11): 5526-5534.

Tang H, Tian B, Brasier AR, Sowers LC and Zhang K (2016) Measurement of Histone Methylation Dynamics by One-Carbon Metabolic Isotope Labeling and High-energy Collisional Dissociation Methylation Signature Ion Detection. *Scientific reports* 6: 31537.

Tian B, Yang J and Brasier AR (2012) Two-step cross-linking for analysis of protein-chromatin interactions. *Methods Mol Biol* 809: 105-120.

Turner BM, O'Neill LP and Allan IM (1989) Histone H4 acetylation in human cells. Frequency of acetylation at different sites defined by immunolabeling with site-specific antibodies. *FEBS letters* 253(1-2): 141-145.

Wajda A, Lapczuk-Romanska J and Paradowska-Gorycka A (2020) Epigenetic Regulations of AhR in the Aspect of Immunomodulation. *International journal of molecular sciences* 21(17).

Woodcock CL and Ghosh RP (2010) Chromatin higher-order structure and dynamics. *Cold Spring Harb Perspect Biol* 2(5): a000596.

Wu MW, L.; Li, Q.; Li, J.; Qin, J.; Wong, J. (2013) The MTA family proteins as novel histone H3 binding proteins. *Cell and Bioscience* 3(1): 14.

Zhang S, Rowlands C and Safe S (2008) Ligand-dependent interactions of the Ah receptor with coactivators in a mammalian two-hybrid assay. *Toxicology and applied pharmacology* 227(2): 196-206.

Zhao R, Nakamura T, Fu Y, Lazar Z and Spector DL (2011) Gene bookmarking accelerates the kinetics of post-mitotic transcriptional re-activation. *Nature cell biology* 13(11): 1295-1304.

Zhao Y and Garcia BA (2015) Comprehensive Catalog of Currently Documented Histone Modifications. *Cold Spring Harb Perspect Biol* 7(9): a025064.

Zheng Y, Thomas PM and Kelleher NL (2013) Measurement of acetylation turnover at distinct lysines in human histones identifies long-lived acetylation sites. *Nat Commun* 4: 2203.

Footnotes

This work was supported by the National Institutes of Diabetes and Digestive and Kidney Diseases grant R01DK122028; and Presbyterian Health Foundation – Harold Hamm Diabetes Center Seed Grant (to A. D. J.). Authors report no conflict of interest.

Figure Legends

Figure 1. Agonist specific dichotomous expression of *stc2* and *cyp1a1*. WT mice were treated with 20 µg/kg of TCDD and 12 mg/kg of CA for the indicated time. RT-PCR was performed to quantitate (A) *cyp1a1* and (B) *stc2* mRNA levels in liver, normalized against 18s ribosomal RNA. For statistical analysis, a mixed-effects multivariate ANOVA (MANOVA) model was used. Following significant overall F test from MANOVA model, the posthoc multiple comparison tests were performed for the prespecified comparisons adjusted by Tukey procedure * $p < 0.05$, $n = 3$ independent mice.

Figure 2. Identification of CA and TCDD specific AhR-associated epigenetic modifications. WT mice were gavaged with 20 µg/kg of TCDD or i.p. with 12 mg/kg of CA for the denoted time period. Cross-linking chromatin immunoprecipitation was performed on livers using anti-AhR antibody followed by LC-MS/MS (xChIP-MS). (A) summarizes mutually exclusive histone modifications detected (denoted by D) upon TCDD and CA treatments at various time-points. * denotes H4 K5 acetylation previously detected by mass spectrometry and western blotting following 2 and 24-hour CA treatment. (B) Representative high-resolution MS/MS spectra of STGG¹⁴K_{ac}APR (encompassing residues 10–17), QLAT²³K_{ac}AAR (residues 19–26), ²⁷K_{me2}SAPATGGVK (residues 27–36) and EIAQDF⁷⁹K_{me}TDLR (encompassing residues 73–83) in histone H3. For CA-specific H4 K5 acetylation, high resolution spectra of G⁵K_{ac}GGKGLGKGGA_KR (encompassing residues 4 – 17 in histone H4) with detailed information regarding theoretical and observed m/z values for fragment ions was published previously (Joshi et al., 2017).

Figure 3. Histone H4 K5 acetylation and H3 K79 methylation at AhR-chromatin complex exclusively upon CA treatment. Cross-linked chromatin immunoprecipitated (with anti-AhR antibodies) protein extracts were subjected to Western blotting and probed with anti-histone modification antibodies. One representative blot is shown (n = 3 independent mice). Histone H3 and H4 were used as loading controls. 0, 5, 10, 15, 30 indicate time in minutes and 1, 2, 4, 6, 8, 12, 24, 48 are hours of 20 µg/kg of TCDD and 12 mg/kg of CA treatment.

Figure 4. Identification of AhR-associated chromatin modification writers of H4 K5 acetylation and H3 K79 methylation. Livers of TCDD and CA treated WT mice were chromatin immunoprecipitated with anti-AhR antibody as described in Materials and Methods. Immunoblotting was carried out to detect enrichment of known histone modification writers of H4 K5 acetylation and H3 K79 methylation. Western blots shown are representative results from 3 independent experiments. 0, 5, 10, 15, 30 indicate time in minutes and 1, 2, 4, 6, 8, 12, 24, 48 are hours of 20 µg/kg of TCDD and 12 mg/kg of CA treatment.

Figure 5. CA-dependent Atf2 and Dot1l binding to stc2 promoter *in vivo*. Chromatin immunoprecipitation (ChIP) assays were performed on livers from WT mice treated with TCDD (20 µg/kg) and CA (12 mg/kg) for 0, 5, 10, 15, 30 minutes and 1, 2, 4, 6, 8, 12, 24, 48 hours. Antibodies against the histone modification writers Atf2, Dot1l and against AhR were used to immunoprecipitate the target proteins. Anti-IgG and anti-H3 antibodies were used as negative and positive controls respectively. PCR using primers

targeting XRE clusters in the *stc2* and *cyp1a1* promoters were used to amplify the precipitated DNA. PCR products were separated on two 5% polyacrylamide gels and visualized with SYBR Green dye. Samples were ran, stained with SYBR Green and imaged on Chemidoc MP (Bio-Rad) simultaneously with exactly same acquisition parameters. Representative images from the ChIP gels are shown. Quantitation of PCR products was performed using ImageLab software (Bio-rad). The bound fraction values were calculated as a percentage of the input DNA used in the immunoprecipitation representing 100% and is shown as mean of %bound from three independent experiments.

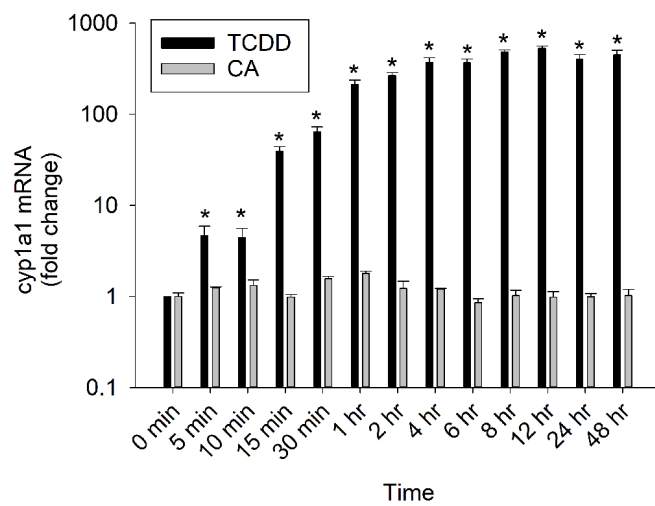
Figure 6. Atf2 and Dot1l are required for the transcription regulation of *stc2*. (A) AML12 cells were transiently transfected with Atf2 and Dot1l siRNAs or Non-Targeting siRNA (NT siRNA). Twenty-four hours later, Western blotting on cell lysates was performed to monitor both Atf2 and Dot1l protein expression. Actin was used as a loading control. (B) AML12 cells, transiently transfected with Atf2, Dot1l and Non-Targeting siRNA for 24 hours were treated with vehicle (DMSO), 6 nM TCDD and 30 μ M CA for 2 hr. Quantitative RT-PCR was performed to measure *cyp1a1* and *stc2* mRNA normalized to 18s rRNA. For statistical analysis, a mixed-effects multivariate ANOVA (MANOVA) model was used. Following overall significant F test from MANOVA model, the posthoc multiple comparison tests were performed for the prespecified comparisons adjusted by Tukey procedure. * $p < 0.05$, $n = 3$ independent batches of AML12 cells. (C). ChIP assays were performed on AML12 cells transiently transfected with targeted and Non-targeted siRNA (NT siRNA) and treated with vehicle, TCDD and CA. PCR products

were loaded onto two 5% polyacrylamide gels (represented by space), ran, stained with SYBR Green and imaged on Chemidoc MP imager (Bio-Rad) simultaneously with exactly identical acquisition parameters. (n = 3 for stc2 and 2 for cyp1a1).

Figure 7. Agonist-specific AhR target gene expression transfers with the gene-specific 'XRE cassette' in the context of chromatin architecture. An edited AML12 cell line was constructed by replacing 926 bp cyp1a1 promoter region containing 10 XREs (between -574 and -1500 bp from transcription start site) with stc2 promoter containing 8 XREs (259 bp region termed 'stc2 XRE cassette' – between -210 to -469 bp from transcription start site) using CRISPR/Cas9 technology. (A) Illustration of cyp1a1 and stc2 promoter regions. Red and blue rectangles represent XREs (5'-GCGTG-3') within cyp1a1 and stc2 promoters respectively. CRISPR/Cas9 edited AML12 cells, where 259 bp stc2 XRE cassette is inserted by replacing cyp1a1 XREs within -574 and -1500 bp is depicted. (B) WT (black bars) and CRISPR/Cas9 edited (grey bars) AML12 cells were treated with vehicle (DMSO), 6 nM TCDD and 30 μ M CA for 2 hr. Quantitative RT-PCR was performed to measure RNA expression of cyp1a1 and stc2 and normalized to 18s rRNA. For statistical analysis, a mixed-effects multivariate ANOVA (MANOVA) model was used. Following overall significant F test from MANOVA model, the posthoc multiple comparison tests were performed by Tukey procedure. *p < 0.05, n = 3 independent batches of AML12 cells. (C) Vehicle, TCDD and CA treated, WT and edited AML12 cells were subjected to chromatin immunoprecipitation using antibodies against AhR, H4 K5ac, Atf2, H3 K79me, Dot1l and H3 (positive control). PCR products were fractionated and visualized on 5% polyacrylamide gels stained with SYBR Green.

Samples were ran on separate gels (represented by space), stained with SYBR Green and imaged on Chemidoc MP imager (Bio-Rad) synchronously with exactly same acquisition parameters (n = 3 independent batches of AML12 cells).

A



B

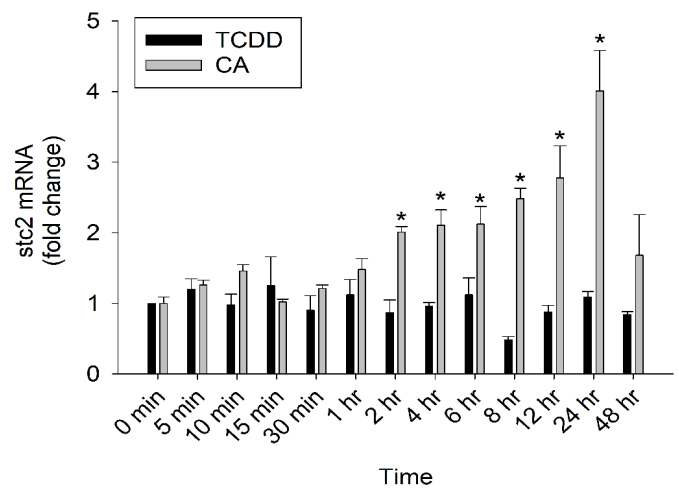


Figure 1

A

PTM /	TIME →	0 min	5 min	10 min	15 min	30 min	1 hr	2 hr	4 hr	6 hr	8 hr	12 hr	24 hr	48 hr
↓ TCDD														
H3 K14 acetylation		-	-	-	-	-	-	-	-	-	-	-	-	D
H3 K23 acetylation		-	-	-	-	-	-	-	D	D	D	D	-	D
H3 K27 dimethylation		-	-	-	-	-	-	D	-	D	-	D	-	D
Cinnabarinic acid														
H4 K5 acetylation*		-	-	-	-	-	-	D	-	-	-	-	D	-
H3 K79 methylation		-	D	D	D	-	D	-	D	D	D	D	D	D

B

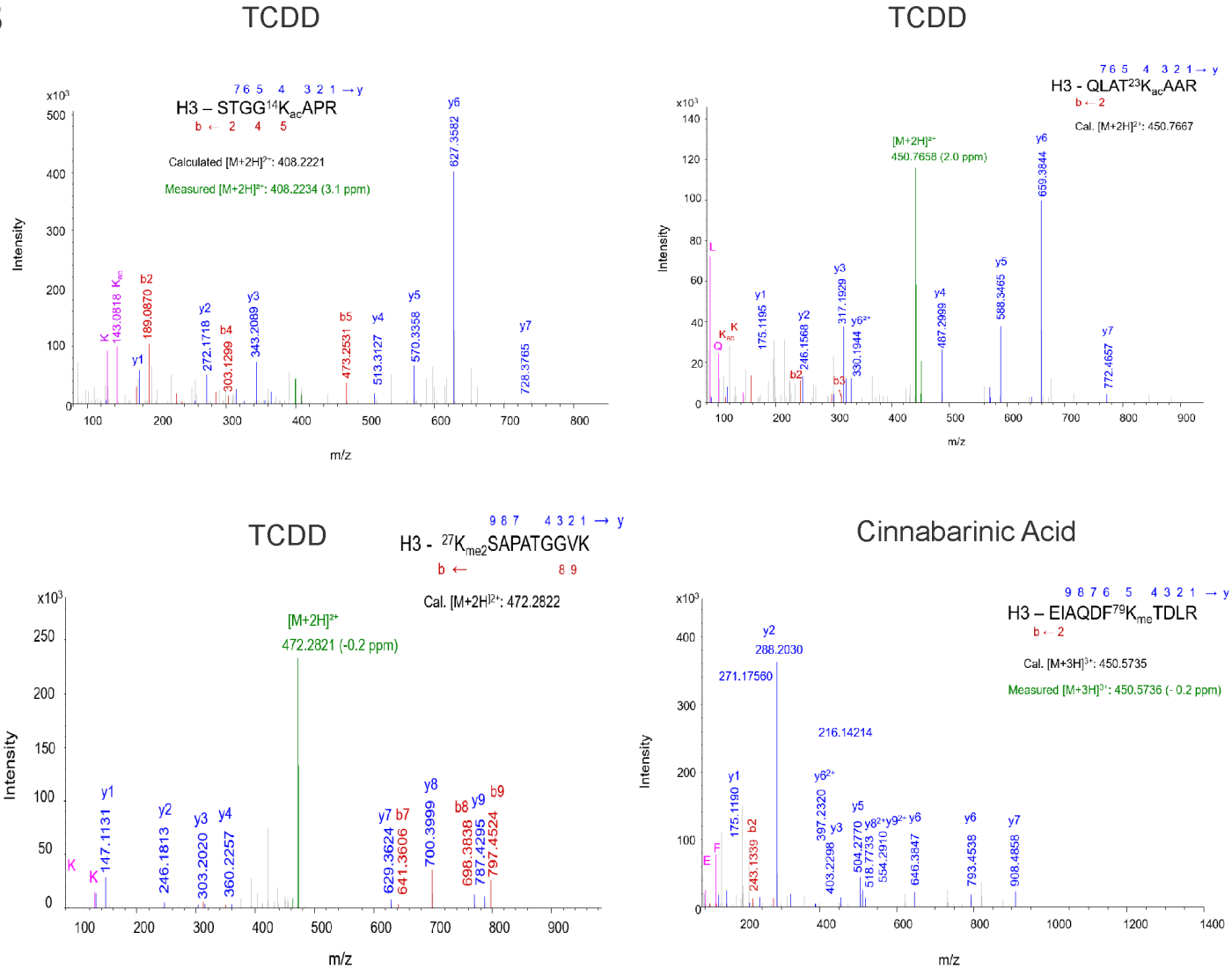


Figure 2

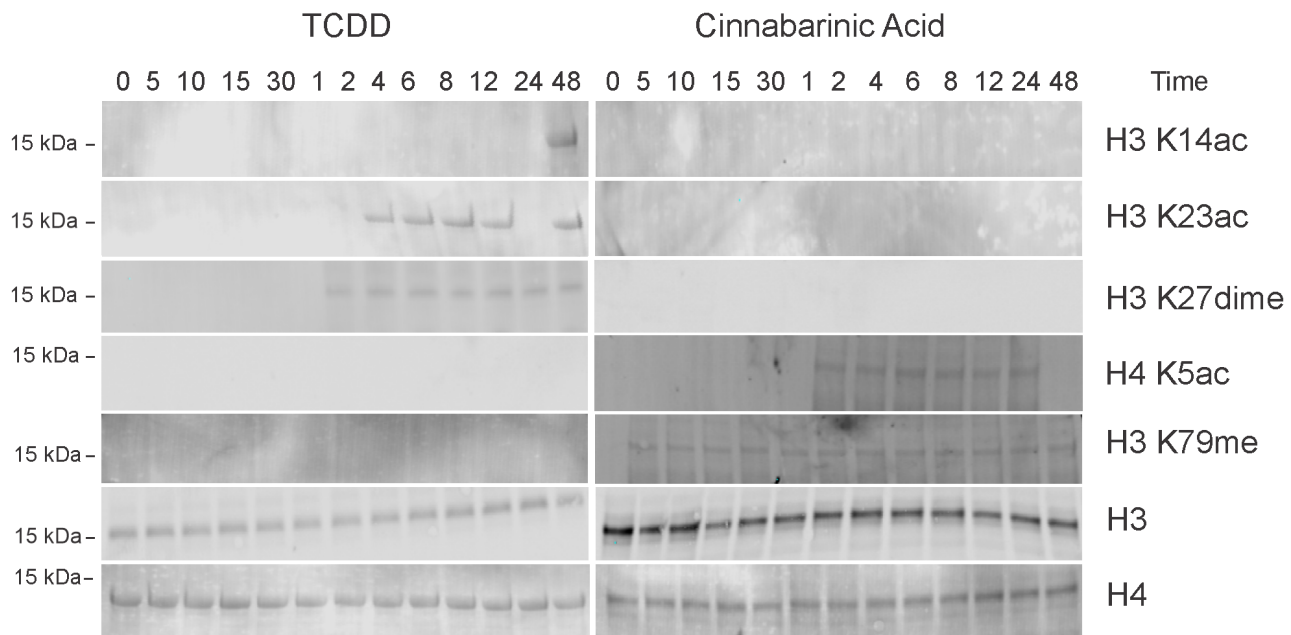


Figure 3

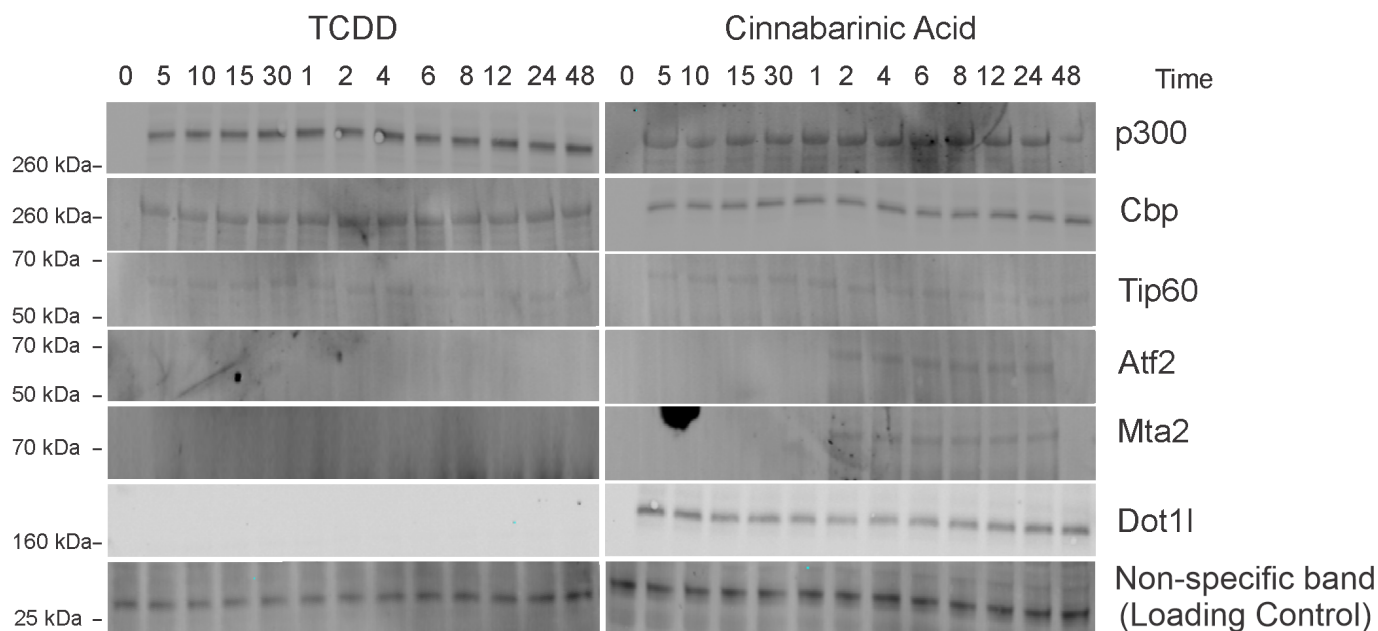


Figure 4

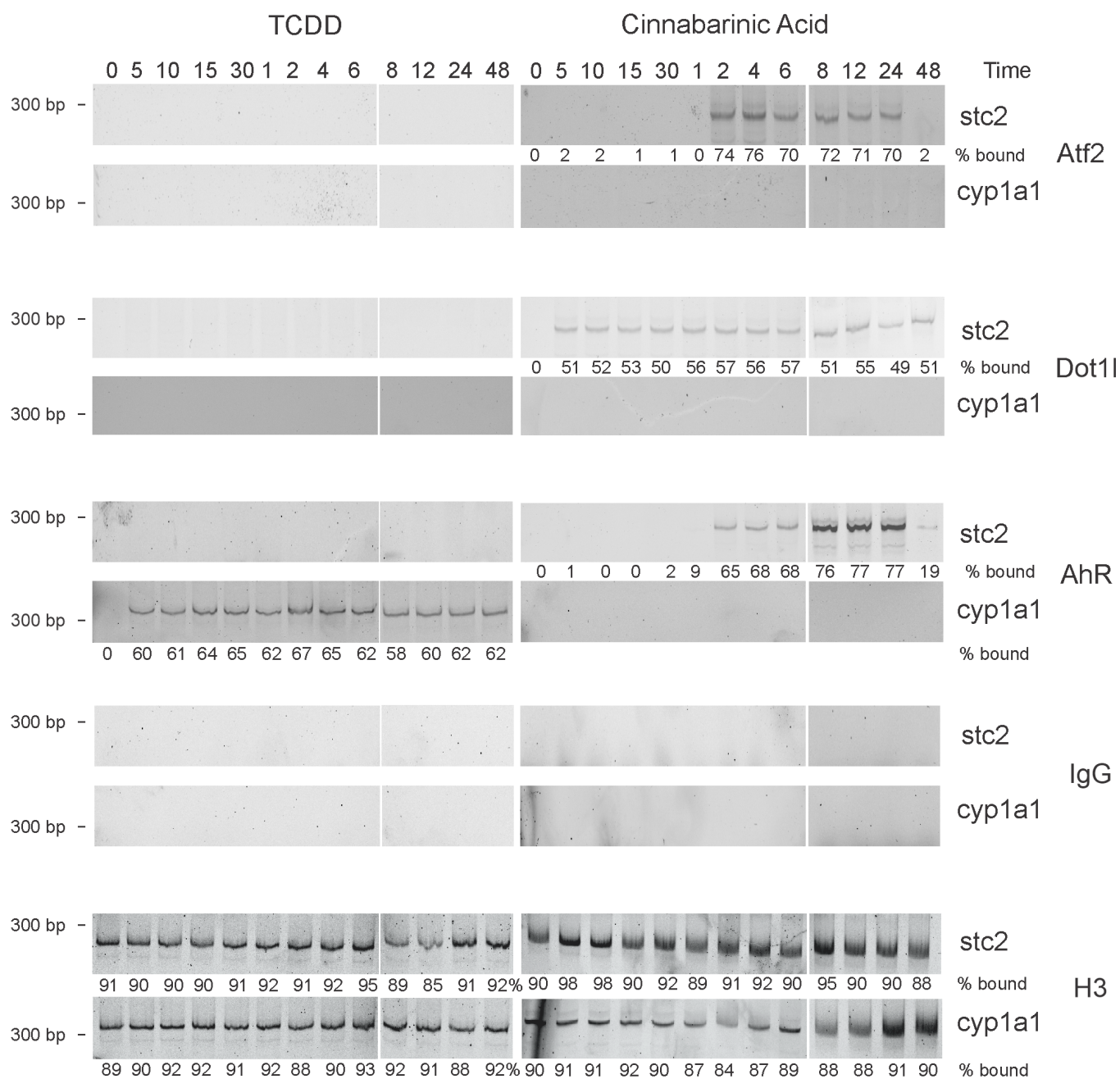


Figure 5

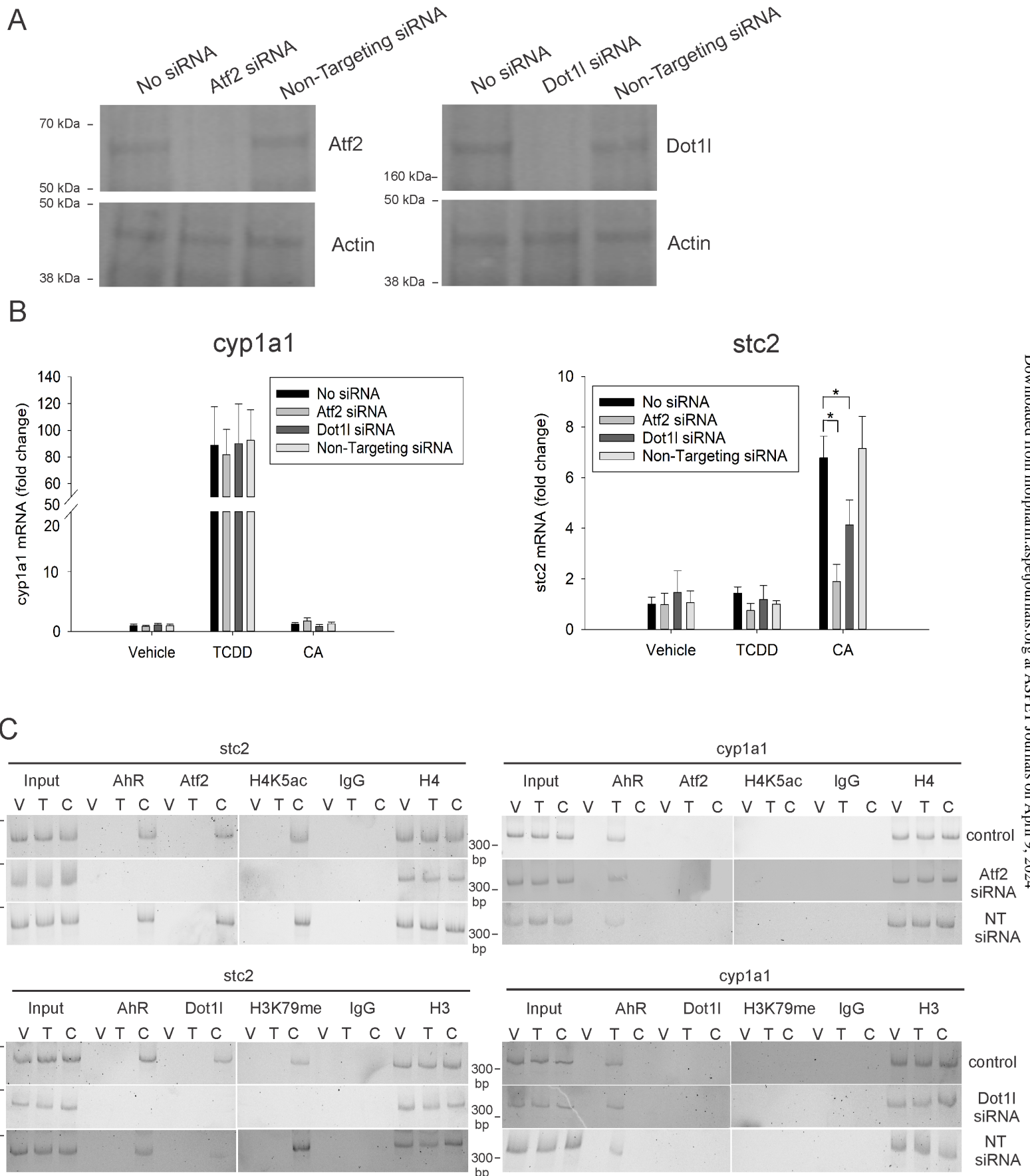
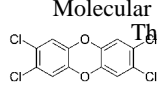


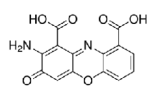
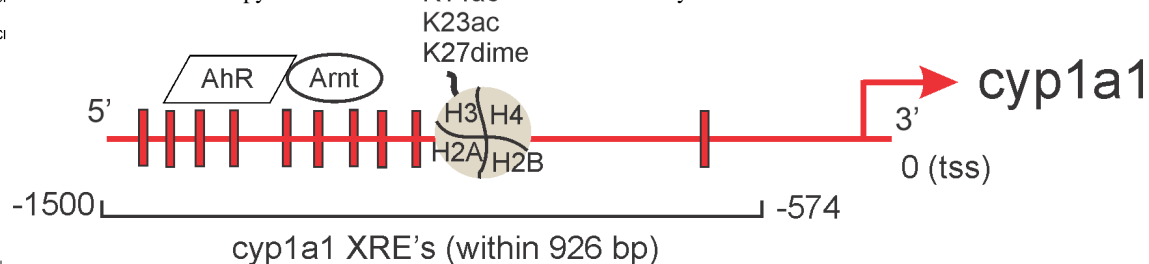
Figure 6

A



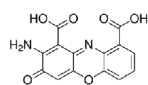
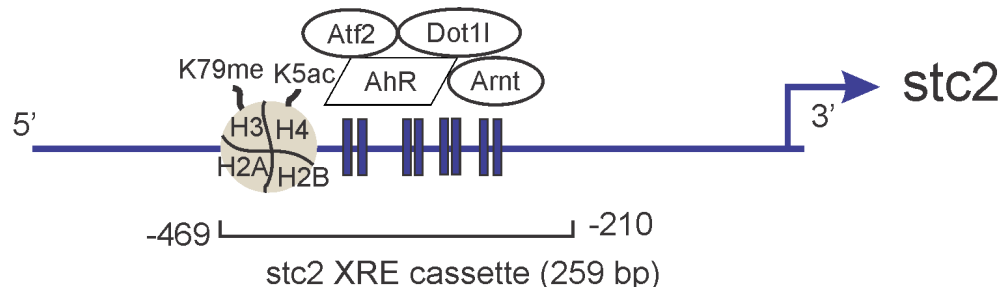
TCDD

WT (*cyp1a1* promoter)



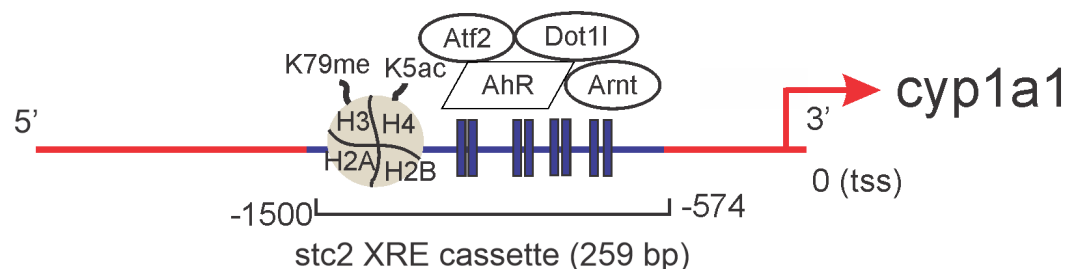
CA

WT (*stc2* promoter)

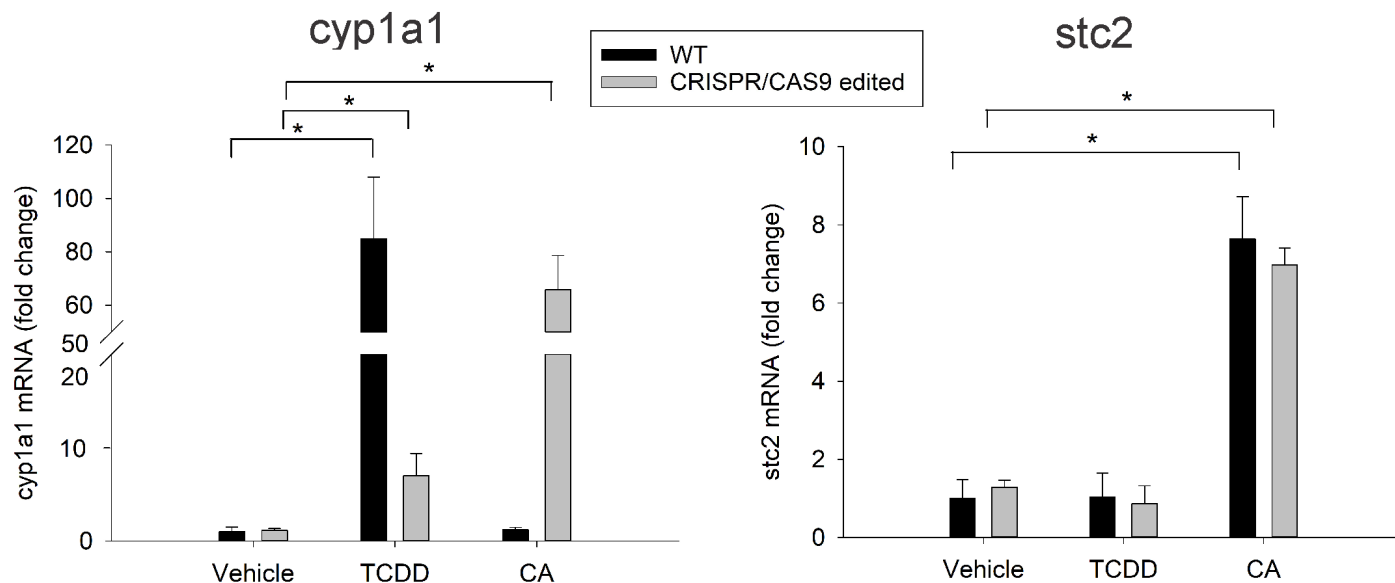


CA

CRISPR/Cas9 edited
(*stc2* XRE cassette in
cyp1a1 promoter)



B



C

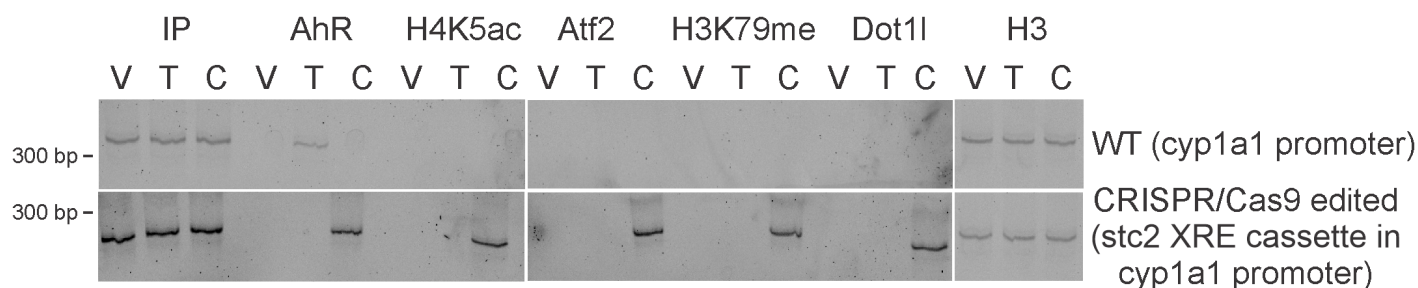


Figure 7

Decoding cinnabaric acid specific stanniocalcin 2 induction by aryl hydrocarbon receptor

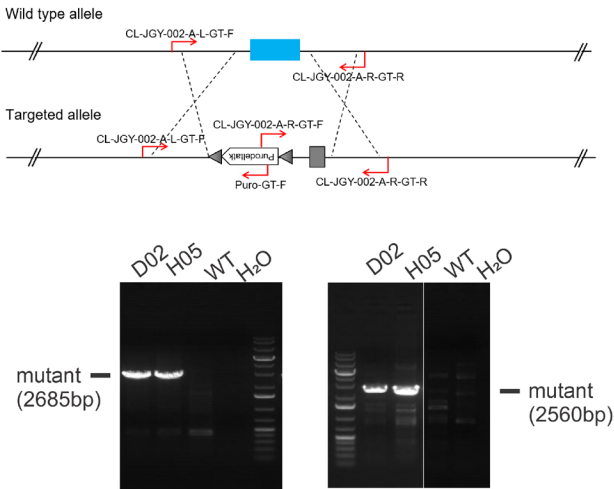
Nikhil Y. Patil¹, Hui Tang², Iulia Rus¹, Kangling Zhang², Aditya D. Joshi^{1*}

Supp. Fig. 1 Junction PCR indicating successful replacement of cyp1a1 promoter XREs with the 'stc2 XRE cassette'. Upon target vector construction, electroporation and puromycin screening; positive clones were selected using junction PCR. Representative gels indicating successful replacement of cyp1a1 promoter XREs with stc2 XREs in clones D02 and H05. Clone D02 is homozygous (cyp1a1 XREs replaced with stc2 XREs in both alleles), whereas H05 is heterozygous with replacement observed in one allele, another allele showed deletion of cyp1a1 promoter region encompassing XREs without insertion of the stc2 XRE cassette.

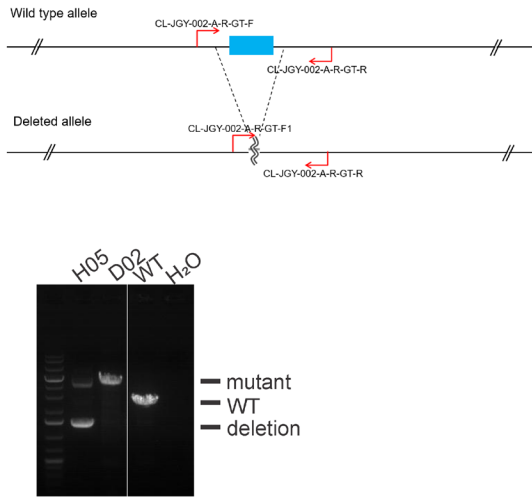
Supp. Fig. 2 Vehicle treatment does not result in target gene induction and histone post-translational modifications. WT mice were treated with vehicle (corn oil) for the indicated time. (A) Quantitative RT-PCR was performed to measure cyp1a1 and stc2 mRNA message. Data is normalized against 18s rRNA and is shown as fold change compared to 0 min vehicle time point. (n = 3 independent mice). (B) xChIP protein extracts were subjected to immunoblotting using anti-histone modification antibodies (n = 2). 0, 5, 10, 15, 30 indicate time in minutes and 1, 2, 4, 6, 8, 12, 24, 48 are hours of vehicle treatment. (C) Western blotting was performed to detect association of known histone modification writers and readers to the AhR complex (n = 2). (D) Chromatin immunoprecipitation was performed on vehicle treated WT mice for 0, 5, 10, 15, 30

minutes and 1, 2, 4, 6, 8, 12, 24, 48 hours. Antibodies against Atf2, Dot1l and AhR were used to immunoprecipitate the target proteins. PCR using primers targeting XREs within cyp1a1 and stc2 promoter were used to amplify the precipitated DNA. PCR products were run on 5% polyacrylamide gel, stained with SYBR Green and imaged on Chemidoc MP (Bio-rad). (n = 3). Representative blots and gels are shown.

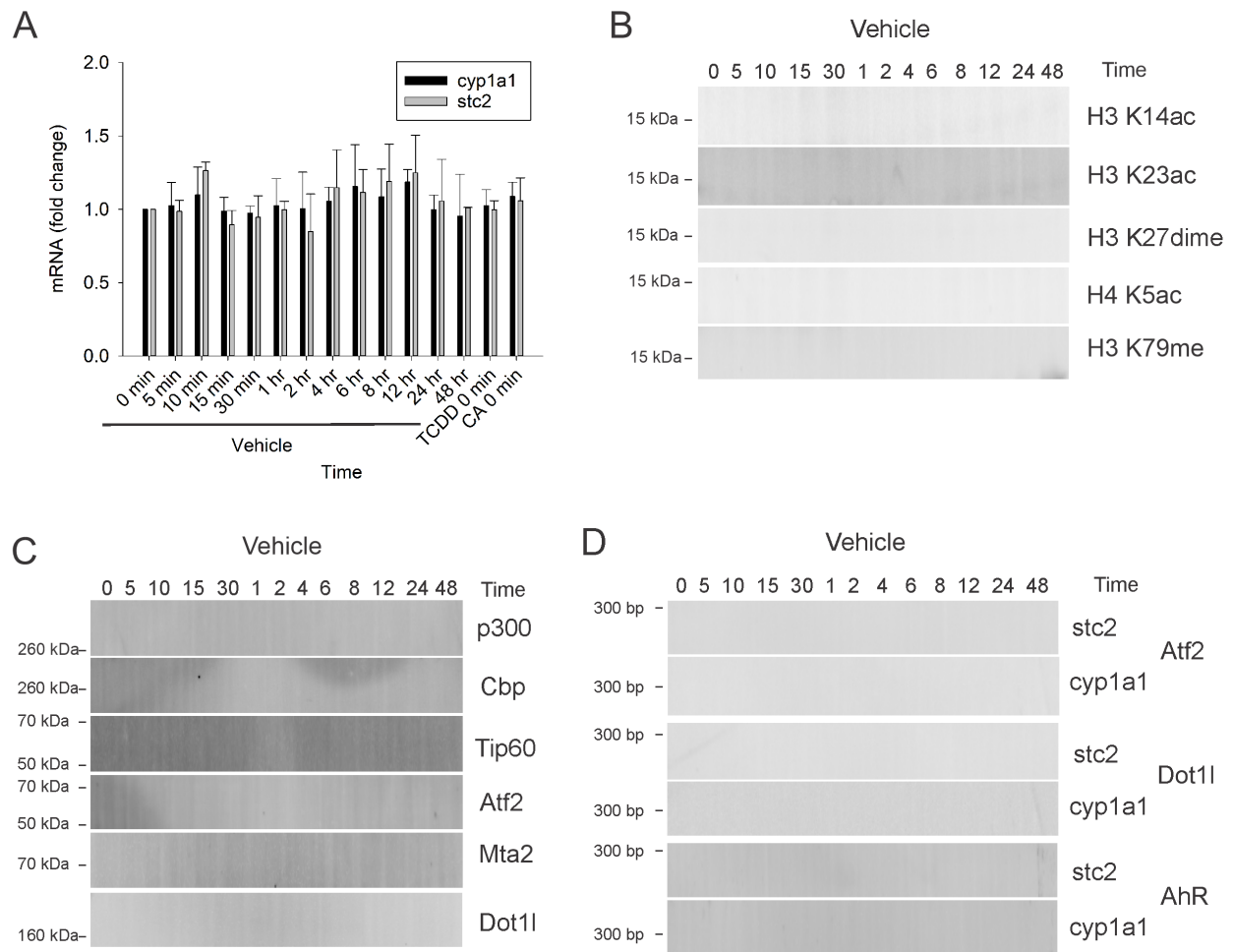
Genotyping Primers: HR allele



Genotyping Primers: non-HR allele



Supp. Fig. 1



Supp. Fig. 2